EAI Endorsed Transactions
on Digital Transformation of Industrial Processes Research Article EAI.EU

A Low-Cost Framework for Textile Yarn Characterization Using Image Processing

Filipe Pereira[1,2,*], Miguel Oliveira[6], Filomena Soares[3], Rosa Vasconcelos[5] and Vítor Carvalho[3,4]

[1] ISEP - Institute of Engineering, Polytechnic Institute of Porto, Rua Dr. António Bernardino de Almeida, 431, Porto, Portugal
[2] MEtRICs Research Center, University of Minho, Campus of Azurém, 4800-058 Guimarães, Portugal
[3] Algoritmi Research Centre, School of Engineering, University of Minho, 4800-058 Guimaraes, Portugal
[4] Ai, School of Technology, IPCA, 4750-810 Barcelos, Portugal
[5] 2C2T Research Centre, School of Engineering, University of Minho, 4800-058 Guimaraes, Portugal
[6] Polytechnic School of Design, Management and Production Technologies Aveiro-Norte, University of Aveiro, Estrada do Cercal, 449 3720-509 Santiago de Riba-Ul, Oliveira de Azeméis, Portugal

Abstract

The textile industry increasingly demands innovative and cost-effective solutions for yarn quality assessment, as conventional equipment is costly and occupies substantial space. This work presents a compact, low-cost image processing framework to characterize key yarn parameters, providing a foundation for future automated quality control systems. The framework employs classical image processing techniques—smoothing, thresholding, segmentation, and morphological operations—implemented with open-source tools such as Visual Studio and OpenCV. An experimental setup using low-cost hardware enabled the acquisition of high-quality images under controlled conditions. The system extracted parameters including linear mass, average diameter, specific volume, defect quantification, hairiness coefficient, and twist direction and pitch. Tests on three yarn types (cotton and polyester) produced results comparable to the industrial reference Uster Tester 3, with error rates below 7%. The proposed solution offers an affordable alternative for small industries and research laboratories, with potential for future integration of advanced computer vision and artificial intelligence to enhance defect detection and classification.

Keywords: Image Processing; Yarn Characterization; Quality Control; Hairiness; Digitalization; Defects; Low-Cost System.

Received on 02 August 2025, accepted on 08 August 2025, published on 12 August 2025

Copyright © 2025 Filipe Pereira *et al.*, licensed to EAI. This is an open access article distributed under the terms of the CC BY-NC-SA 4.0, which permits copying, redistributing, remixing, transformation, and building upon the material in any medium so long as the original work is properly cited.

doi: 10.4108/dtip.9821

* Corresponding author. Email: fal@isep.ipp.pt

1. Introduction

The textile industry is a critical sector of the global economy, where yarn quality directly influences the final characteristics of textile products, including strength, aesthetics and durability. Traditionally, yarn quality control has largely relied on advanced industrial equipment such as the Uster Tester series, which, although very accurate, are expensive, complex, use capacitive or optical sensors, and lack portability [1-4]. These limitations make it difficult to use at laboratory or industrial levels, especially in small and medium-sized enterprises and academic environments. Recent advances in computer vision and image processing have enabled new opportunities for the development of more compact and cost-effective solutions for industrial quality control [5–8]. However, within the textile industry, research still focuses mainly on the detection of isolated defects or the evaluation of very specific parameters, lacking more comprehensive systems capable of performing the analysis of mass, defect and statis-tical parameters in yarns [9-12].

In this context, the present work proposes a compact, modular and low-cost image processing framework for a more comprehensive characterization of yarns. The main objectives include: (1) designing a dedicated image acquisition system using affordable hardware; (2)

implement classical image processing techniques such as smoothing, thresholding operations, segmentation, and morphological operations, to accurately extract yarn parameters; and (3) validate system performance on industrial equipment using different types of yarns.

This work proposes a low-cost and novel framework for image processing that is cost effective and compact which can serve as a building block for future developments in assessing the quality of textile yarn. This includes possible interfacing with machine vision and AI systems.
The main findings are:

(i) Development of a structure with possible industrial integration, academic labs, small manufacturers, teaching environments and low cost for yarn characterization.
(ii) Application of image processing techniques (filtering, segmentation, morphological operations) to accurately extract yarn quality parameters.

The implication of the main finding?
(i) Allow the use of a cost-effective alternative in an industrial environment for yarn quality control.
(ii) Serve as a working foundation for future improvements using more advanced AI-based computer vision and inspection systems.

Compared to conventional industrial systems, the proposed solution offers the following practical and scientific advantages:

- Cost-effective and affordable: built with low-cost hardware and open-source software (Visual Studio and OpenCV), making it suitable for small and medium-sized textile industries, research centers and educational institutions.
- Portability and ease of implementation: its compact design facilitates integration into laboratory and industrial environments, without requiring very complex infrastructures.
- Modularity and future scalability: The system architecture allows for easy upgrades and adjustments, enabling future integration of more advanced computer vision and artificial intelligence techniques to improve defect detection and classification.
- Very comprehensive analysis of several parameters: the system created allows to obtain with some precision the critical parameters of yarn mass quality, such as linear mass, average diameter, specific volume, quantification of defects (fine points, thick points, neps), hairiness coefficient and twist analysis, within a single structure.
- Compared to other approaches published in this area, this work introduces a platform that, despite its technical simplicity, represents a significant advance in terms of immediate practical applicability, especially for:
    - Small and medium-sized companies;
    - Academic laboratories and educational institutions;
    - Environments where the cost, complexity and space occupied by conventional commercial solutions severely limit their adoption.
- Contribution to Industrial Digitalization 4.0: This system will enable companies to digitally transform the textile industry by providing a scalable and low-cost quality control solution.

The results demonstrate that this system represents a viable and cost-effective alternative to expensive industrial solutions, allowing its use in yarn quality control in academic and industrial environments, and laying the foundation for future developments in intelligent textile inspection.
The following chapters are structured as follows: Chapter 2 presents the essential theoretical concepts for the characterization of the textile yarn, followed by a detailed literature review and a comparative analysis of existing solutions. Chapter 3 describes the materials and methods used in the development of the proposed framework, including experimental setup and image processing techniques. Chapter 4 discusses the results obtained, providing a critical analysis of the system performance compared to industrial standards. Finally, Chapter 5 summarizes the main conclusions of the work and describes possible future research directions to improve and extend the proposed system.

2. Theoretical concepts and state of art

2.1. Yarn characterization parameters

Hairiness, being an important characteristic of yarn quality, is defined by the number of fibers that protrude from the yarn core. This feature directly affects the visual appearance, tactile feel, and durability of textile products. Hairiness is typically categorized into two main types: loop fibers, which are anchored at both ends within the yarn core, and protruding fibers, which are attached at only one end and extend freely from the yarn body. These morphological differences have a very significant impact on yarn processing and performance. Another important parameter is yarn twist, which results from the rotational motion applied during yarn production. The twist direction can be classified as S-twist or Z-twist and significantly influences the strength, flexibility, and behavior of the yarn during fabric formation [14-21].
In addition to these properties, yarn defects such as fine spots, coarse spots, and neps influence the uniformity and quality of textile products. Traditionally, yarn quality characterization and assessment are performed using capacitive and optical sensors or through the use of industrial equipment such as the Uster Tester and the Uster Zweigle HL400. Despite their widespread use, these systems are associated with high acquisition and maintenance costs, operational complexity, and lack of

portability, limiting their accessibility, especially in small and medium-sized companies and academic environments [13]. In response to these limitations, there is a growing demand for more accessible, cost-effective, and efficient solutions for yarn characterization. Recent technological advances have led to the development of alternative systems based on computer vision and image processing techniques. These systems are capable of performing automated and non-destructive assessments of yarn properties, which allows for advantages in terms of portability, ease of integration, and reduced costs. Furthermore, these solutions lay the foundation for future improvements through the integration of artificial intelligence and advanced computer vision technologies, contributing to the digitalization and modernization of the textile industry within the framework of Industry 4.0 [14-21].

2.2. Literature Review and comparative analysis

In recent years, several researches have focused on improving yarn quality characterization methods using computer vision and advanced image processing techniques. However, many of these solutions remain limited to very specific parameters and sometimes only obtain 1 or 2 parameters [14-31]. They also depend on very expensive or complex hardware and require very high computational resources. Table 1 below presents a comparative analysis of the main existing systems and highlights how the current work addresses the limitations found in the literature.

Table 1. Comparison of existing systems and addressed limitations..

System	Measurement Approach	Key Parameters Extracted	Main Limitations
Qiu et al., 2024 [22]	Hairiness on Yarn Cones using Computer Vision (Online, Nondestructive)	Hairiness Index (Hp), Total Hair Length	Focus only on hairiness; requires specific conveyor setup; no mass or twist analysis
Guo et al., 2023 [23]	Hairiness on Sizing Yarn (Online, Computer Vision with Adaptive Thresholding)	Hair Length Index; Robustness to yarn variety and imaging conditions	Specific to sizing yarn; limited to hairiness; no mass or twist evaluation
Pereira et al., 2025 [24]	Image Processing + Deep Learning (YOLOv5s6, Detection of Loop and Protruding Fibers)	Hairiness, Loop and Protruding Fibers, Defects, Spectrogram, Twist, Mass	High computational complexity; requires AI expertise
Pereira et al., 2023 [25]	Image Processing + AI, Real-Time Hairiness and Mass Parameters Analysis	Hairiness, Linear Mass, Diameter, Volume, Twist, Defect Detection, Spectral Analysis	Complex system; costly hardware; larger physical footprint
Zhang et al., 2023 [26]	L0 norm smoothing and Expectation Maximization method	Apparent evenness, diameter CV	Focused only on diameter evenness; no twist orientation or step analysis; not real-time.
Zhang et al., 2024 [27]	Modified Canny edge detection	Apparent evenness, yarn diameter	Limited to 2D edge contours; does not capture twist, mass, or hairiness information
Li et al., 2016 [28]	Yarn image sequence analysis over time	Diameter variation (apparent unevenness)	No analysis of twist orientation or pitch; depends on stable frame sequence; not suitable for real-time
Wang et al., 2016 [29}	Multi-perspective mirrored image acquisition	Hairiness (multi-view profile)	Twist and mass evaluation not included; complex

			optical setup; no structural analysis
Zhou et al., 2024 [30]	Deep learning segmentation (multiscale and boundary-assisted)	Curve-like fiber structures	High computational complexity; twist orientation and pitch not evaluated; no physical parameter extraction
Yu et al., 2023 [31]	3D low-cost multi-camera setup + signal processing	3D unevenness, diameter variability	Does not measure twist orientation or step; requires synchronized cameras and calibration; limited portability

Recent yarn characterization methods have focused on increasing accuracy and automation through advanced computer vision techniques, including deep learning, multi-scale segmentation, and multi-camera 3D acquisition systems. However, as summarized in Table 1, these approaches focus on very few yarn properties, such as diameter or hairiness, often requiring complex hardware, complex calibration procedures, or high-performance computational resources. These constraints limit their accessibility and integration in smaller industrial environments or academic laboratories.

On the other hand, the solution presented in this work offers a balanced and affordable alternative, combining multiple yarn quality metrics in a single, compact, and low-cost system, based on open-source tools and classical image processing techniques.

The main advantages of the current work compared to existing solutions are:

(i) Low Implementation Cost: It uses accessible and low-cost hardware and open-source software, allowing implementation in small and medium-sized companies in the industry, research environments, universities and laboratories.

(ii) Portability and Simplicity: The compact design of the system allows easy integration without the use of more complex infrastructures or those that require higher computational resources.

(iii) Comprehensive Parameter Analysis: Unlike most of the reviewed works, this one evaluates multiple key parameters simultaneously, including linear mass, diameter, volume, twist and hairiness coefficient.

(iv) Foundation for Future Expansion: The modular architecture facilitates the future integration of AI and advanced computer vision techniques.

(v) Non-Destructive and Automated Measurement: Provides objective and re-liable measurements, preserving the integrity of the yarn samples.

(vi) Dedicated Image Processing Framework: A framework was developed for image processing, including well-defined acquisition, pre-processing, seg-mentation and feature extraction steps. This ensures accurate extraction of parameters while maintaining computational efficiency.

(vii) Good integration in industries environments.

(viii) Use of Classical and Effective Image Processing Techniques: Techniques such as spatial filtering, thresholding, morphological operations and contour analysis were applied to obtain detection of yarn characteristics without the need for more advanced computational resources.

In the following chapter, the proposed hardware architecture and the specific image processing techniques implemented within the developed framework are presented.

3. Materials and methods

The first phase of the entire methodology focuses on defining the digital image acquisition system for subsequent processing. The definition of this system is based on the construction of a simple and accessible prototype that allows validating the application of the image processing technique for extracting textile yarn quality parameters. Figure 1 shows the schematic of the system designed for digital image acquisition.

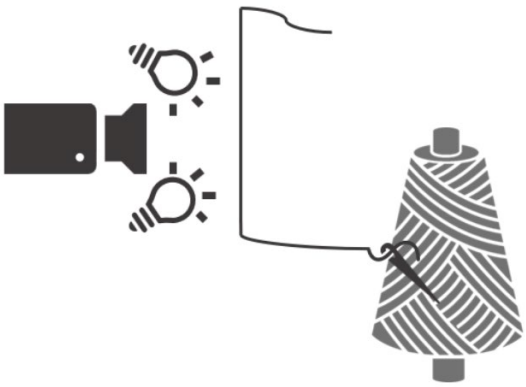

Figure 1. Design of the image acquisition system

Regarding the quality factors of the image acquisition system, Table 2 summarizes the definition of the parameters working distance, magnification and camera height.

Table 2. Definition of image acquisition system parameters.

Yarn type	Working Distance	Magnification	Camera Height
PURPLE COTTON	4.50MM	868X	65,0 MM
YELLOW COTTON	5.00MM	890X	65,0 MM
WHITE POLYESTER	4.50MM	868X	65,0 MM

The working distance and camera height are determined using the previously described methodology [24]. Although the magnification is typically calculated using the focal length and sensor size, these specifications were not provided for the generic USB camera used.
Instead, magnification was adjusted manually using the camera's adjustable ring, which controls magnification between 50X and 1000X. This ring is divided into 43 sections, meaning each section adjusts magnification by approximately ±22X, as calculated by:

$$\text{Magnification per Section} = \frac{1000X - 50X}{43} = \pm 22\text{X} \qquad (1)$$

Given the small size of the yarn samples, a high magnification was required, which was manually set by adjusting the ring until achieving a sharp, high-resolution image without optical blur.

3.1. Hardware and Software - Image Acquisition System Definition

The system developed for characterization of textile yarns was designed with a focus on low cost, simplicity and portability, ensuring good image quality for accurate parameter collection. The image acquisition process plays an important role in capturing clear and consistent images of yarn samples, directly influencing the processing efficiency of the following steps.
The system consists of a low-cost USB microscope camera equipped with an integrated LED ring illumination system that provides uniform and stable illumination. The camera specifications are shown in Table 3.

Table 3. Main Technical Specifications of the Camera.

Feature	Specification
MODEL	USB DIGITAL MICROSCOPE CAMERA
INTEGRATED LIGHTING	8 ADJUSTABLE LED LIGHTS
IMAGE RESOLUTION	640 × 480 PIXELS
OPTICAL MAGNIFICATION	VARIABLE FROM 50X TO 1000X
MAXIMUM FRAME RATE	30 FRAMES PER SECOND (FPS)

To minimize the influence of external light sources and environmental variations, the image acquisition setup was installed inside a closed black box, ensuring controlled lighting conditions and reducing reflections or shadows.
A simple mechanical structure, using ceramic guides and adjustable supports, was developed to keep the wire under controlled tension and aligned within the camera's field of view.
This ensured that the wire remained fixed during image acquisition, preventing movement drift and also allowing consistent measurements across all captured images.
Image acquisition was managed using SENTECH StViewer software, which allowed manual control of camera settings such as exposure time, brightness and focus.
Images were saved in a standardized format and subsequently processed using an application developed in Visual Studio (C#), integrated with the OpenCV library for image processing operations.

3.2. Yarn samples

Three types of textile yarns were used: purple cotton yarn, yellow cotton yarn and white polyester yarn, as shown in Figure 2. The samples are placed in the development system, where the data is processed using the algorithm that was developed. Finally, the results are made available, analyzed and compared with the values read by the Uster Tester 3. In this sense, it is possible to conclude on the capacity and feasibility of applying image processing techniques to determine quality parameters of textile yarns. In addition, temperature and humidity control is also implemented during the testing phase.

Figure 2. Types of textile yarn used in work – purple cotton, yellow cotton and white polyester yarn.

3.3. Developed Prototype

The validation of the image processing techniques was performed using a physical prototype described in Subchapter 3.1. The system consists of the textile yarn under analysis, a low-cost USB microscope camera with integrated LED illumination, a separate LED ring, a spool to store the analyzed yarn, and a black enclosure to create a controlled environment.

Sample acquisition was divided into two phases:

- **Phase 1:** 500 images were captured to analyze linear mass, mean diameter, specific volume, defect quantification, and hairiness coefficient. This larger sample size ensured an accurate comparison with the USTER Tester 3.
- **Phase 2:** 50 images were captured to analyze twist direction and pitch, since these parameters are not evaluated by the USTER Tester 3. This phase focused on validating the repeatability of the developed system.

During testing, the wire was positioned horizontally and parallel to the camera, maintaining a constant working distance to ensure image clarity and measurement accuracy. The wire was tensioned and wound onto an empty spool, which allowed for controlled movement and positioning during image capture. An external light source, positioned parallel to the camera and the wire, allowed for adjustable illumination based on the needs of the yarn analysis.

Figure 3 illustrates the complete image acquisition setup.

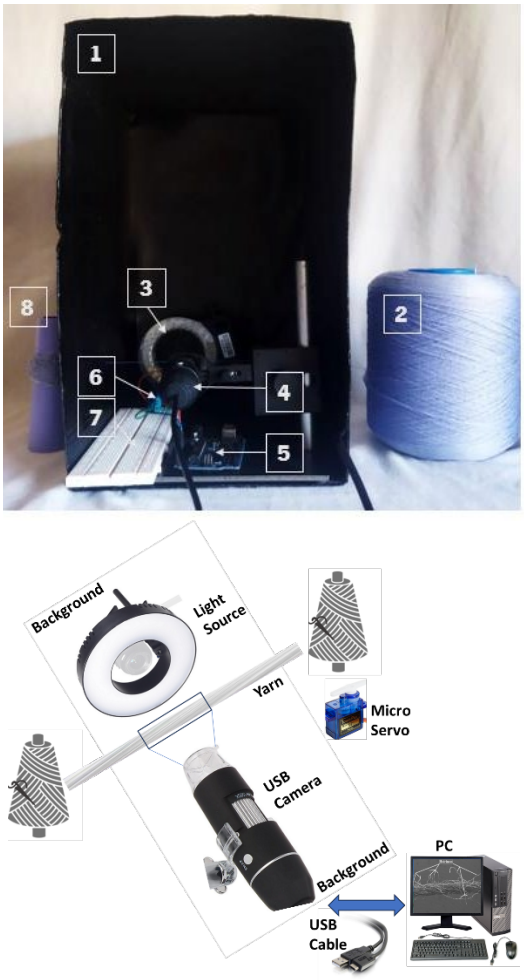

Figure 3. Prototype of the image acquisition system (left), and schematic diagram illustrating the component layout and acquisition geometry (right). Legend of left image: 1 – Black Enclosure; 2 – Textile Yarn Bobbin for Analysis; 3 – LED Ring; 4 – Generic USB Camera; 5 – Arduino Uno Microcontroller; 6 – DHT11 Sensor; 7 – Breadboard; 8 – Analyzed Textile Yarn Bobbin

3.4. Algorithm Application and Yarn Parameterization

The image processing algorithm was developed in Visual Studio, using the OpenCV library to simplify complex image manipulation operations. This algorithm handles the entire image processing workflow.

The procedure begins with loading a color image into the development environment. If the image is not found in the specified path, the system displays an error message.

The results are displayed in the development console and automatically stored in structured tables, which are then exported to Microsoft Excel. The data organization follows two phases:

- **Phase 1:** Samples are identified as Yarn A (purple cotton), Yarn B (yellow cotton), and Yarn C (white

polyester), labeled sequentially (e.g., A1, A2…). Parameters such as average diameter, linear mass, specific volume, defect count (thin places, thick places, neps), and hairiness coefficient are calculated.

- **Phase 2:** For twist analysis, samples are numbered from 1 to 50, and the majority twist direction and twist pitch average are determined for each sample.

To ensure adequate testing conditions, a simple temperature and humidity monitoring system was developed using a low-cost microcontroller (Arduino Uno) and a DHT11 sensor. This avoided the need for expensive industrial controllers, while maintaining the focus on low system cost while still providing adequate environmental monitoring during data acquisition.

3.5. Initial definition of image processing techniques

After image acquisition, it was processed on a development platform to allow data extraction. This phase involved several techniques such as image enhancement, analysis and coding. The methodology developed focuses specifically on image analysis to meet the project objectives. The strategy follows a sequence of small processing steps to progressively reduce image noise, ensuring cleaner and more relevant data for analysis. This process is illustrated in Figure 4, which describes the general procedure for initial image processing.

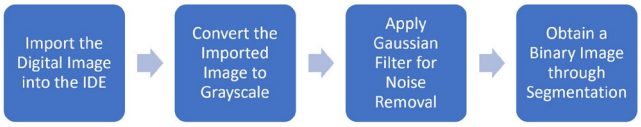

Figure 4. Diagram of the initial processing of the digital image.

The initially captured image is in color, requiring grayscale conversion to simplify the processing workflow. This conversion eliminates the complexity introduced by color and reduces computational effort, facilitating the next phase of image segmentation [32-35]. After grayscale conversion, a Gaussian filter is applied to remove noise [32-35]. This filtering step eliminates irrelevant information by smoothing out abrupt changes in intensity between pixels, resulting in a slightly blurred image that focuses on the essential features for parameter analysis. In addition, it prepares the image for linearization in the next step.

Although the visual differences before and after the application of the Gaussian filter [32-35] may seem minimal, this process correctly reduces abrupt variations in pixel intensity, as illustrated in Figures 5a and 5b.

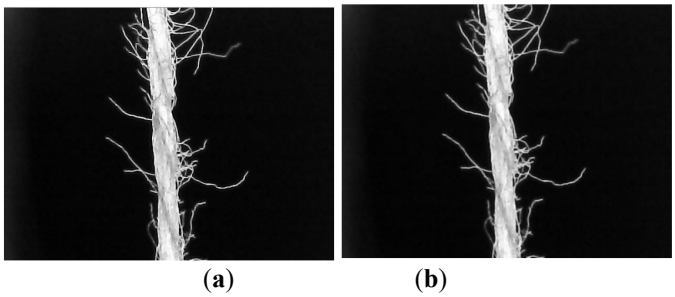

Figure 5. Image processing techniques: (a) Conversion of the initial color image to grayscale; (b) Application of the Gauss filter to remove the initial noise.

Next, image segmentation is performed to group the pixels based on their intensity values. Two subgroups are created: one for pixels with intensity 0 (black) and another for pixels with intensity 1 (white). Essentially, a binary image is generated from the grayscale image, clearly separating the wire from the background [36].

This process relies on defining a threshold value, which can be set manually or automatically. If the intensity of a pixel is below the threshold, it is set to 0 (black); if it is above, it is set to 1 (white). To automate this process, the Otsu algorithm is applied. This method automatically determines the optimal threshold value (between 0 and 255 for 8-bit grayscale images) by correctly dividing the pixel intensity levels to achieve accurate segmentation [37–40].

The segmentation step is based on the Otsu method, which automatically determines the optimal threshold to separate the foreground from the background based on the histogram distribution of pixel intensities [40,61]. This binarization process is applied after Gaussian filtering and grayscale conversion (Figure 6), resulting in a binary image that isolates the yarn from the background. This approach is effective under controlled imaging conditions, i.e., a closed acquisition chamber with uniform LED illumination, which decreases contrast variability. However, for other tasks (such as torsion analysis), a fixed threshold value of 200 was manually selected to improve contrast on specific features.

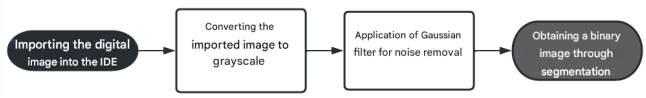

Figure 6. Initial image processing phase: (a) Converted image; (b) Result of applying the Otsu algorithm to obtain a binary image.

The final result of this initial image processing phase is shown in Figure 7a and 7b, illustrating the binary image obtained after applying the Otsu algorithm [40].

The samples analyzed in this study correspond to multifilament textile yarns, composed of fibers twisted together to form a single yarn. Thus, the analysis performed corresponds to the "yarn twist" parameter, defined as the

internal twist between the component fibers. The term "strand twist", on the other hand, typically applies to single-strand yarns grouped together to form cables or ropes, and does not apply to the structure under analysis.

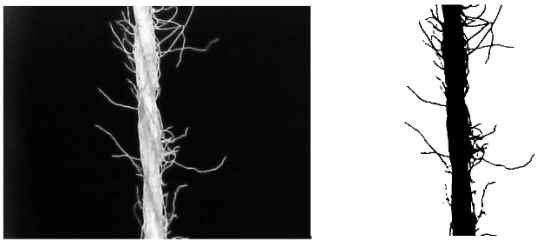

Figure 7. Initial image processing phase: (a) Converted image; (b) Result of applying the Otsu algorithm to obtain a binary image.

3.6. Procedure for extracting textile yarn parameters

After initial processing, the hairiness is removed to isolate the yarn core, allowing the extraction of mass parameters such as mean diameter, linear mass, specific volume and defects.

To calculate the diameter, a morphological closure operation is applied to eliminate noise and residual fibers, leaving only the yarn core. This operation combines dilation and erosion techniques to fill gaps in the binary image and prepare it for more accurate measurements [41]. Figure 8 shows the result of this process.

Figure 8. Result of applying the morphological closing operation.

In the final stage of image processing, a low-pass filter is applied to remove residual high-frequency noise [42] and preserve the relevant low-frequency components of the yarn. This is done through a convolution process with a new kernel, resulting in a cleaner image with a thinner yarn kernel, as shown in Figure 9.

Figure 9. Result of applying a filter to remove residual noise.

Figure 10 represents a flowchart that summarizes the methodology performed.

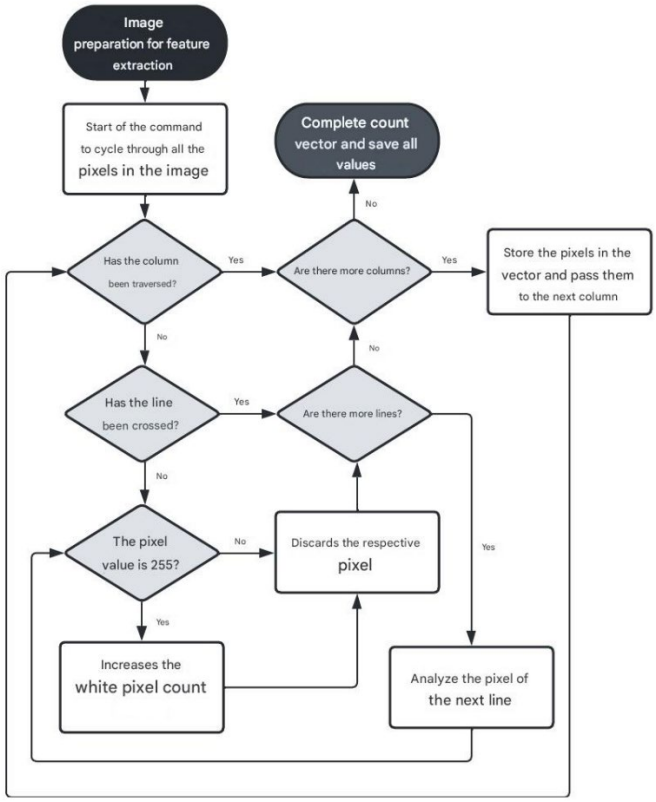

Figure 10. Flowchart of the methodology applied to obtain the diameter.

The linear mass is calculated directly from the average diameter. Similarly, the specific volume is obtained after calculating the linear mass [36-45].

No special methodology is required for these calculations; only the material's density and porosity must be defined. For this project, cotton and polyester densities were used (1.52 g/cm³ and 1.34 g/cm³, respectively), and porosity was assumed as the average value of the typical range (0.55–0.70) [52].

3.7. Procedure for obtain defects

Three types of yarn defects are identified: thin places, thick places, and neps, determined based on variations in linear mass along the yarn. The sample is divided into five sections, and for each, the average diameter and corresponding linear mass are calculated [24].

The classification follows this logic:

- If linear mass is less than 50% of the average → Thin Place.
- If linear mass is more than 50% of the average → Thick Place.
- If linear mass is more than 200% of the average → Nep (aligned with USTER Tester 3 criteria).

Finally, the total count of each defect type and the Imperfection Index (IPI) and the sum of all defects per kilometer is calculated [46,47]. The process is illustrated in Figure 11.

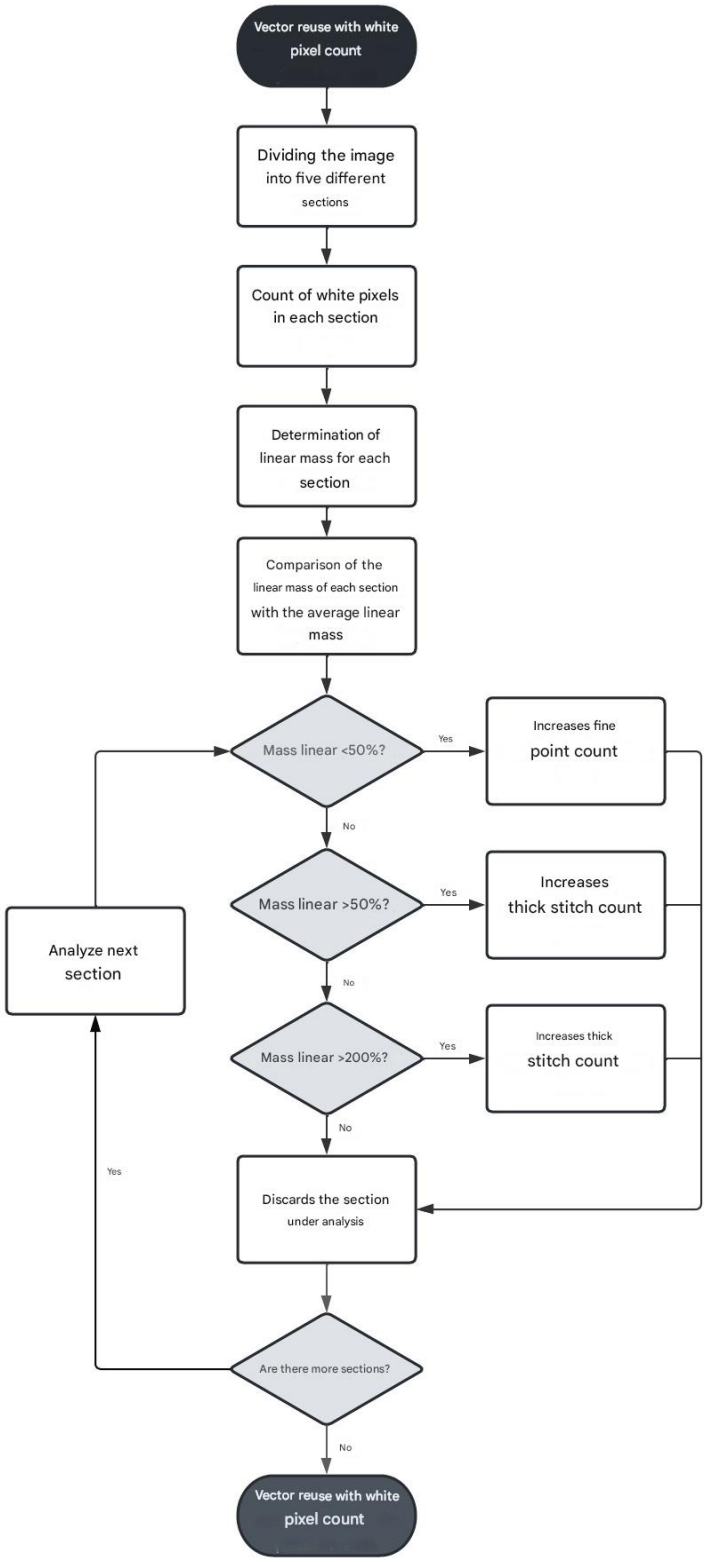

Figure 11. Flowchart of the methodology applied to obtain different types of defects.

3.8. Coefficient of hairiness

The hairiness coefficient quantifies the amount of loose fibers along the yarn, distinguishing between protruding fibers (attached at one end) and loop fibers (attached at both ends) [48]. While previous parameter calculations required removing these fibers, calculating the hairiness coefficient involves specifically analyzing them.
To highlight loose fibers, an additional processing step is applied:

- A morphological dilation enlarges the yarn core boundaries by adding white pixels (Figure 12).
- The dilated image is subtracted from the original binary image, isolating the hairiness region.

A skeletonization (thinning) operation is then applied to simplify the image and represent the fibers as thin structures, reducing area redundancy and facilitating accurate fiber length measurement.
This process ensures reliable calculation of the hairiness coefficient by minimizing errors caused by overlapping or excessive fiber areas.

Figure 12. Dilation of the nucleus individualized in the previous stage.

The dilated image is subtracted from the binary image to remove the yarn core, isolating only the hairiness region. A skeletonization (thinning) process is then applied, simplifying the fiber shapes into thin lines that retain essential morphological information [49].
This reduces image complexity and prevents errors in fiber length measurement, allowing accurate calculation of the hairiness coefficient. Figures 13a and 13b illustrate the subtraction and skeletonization results, respectively.

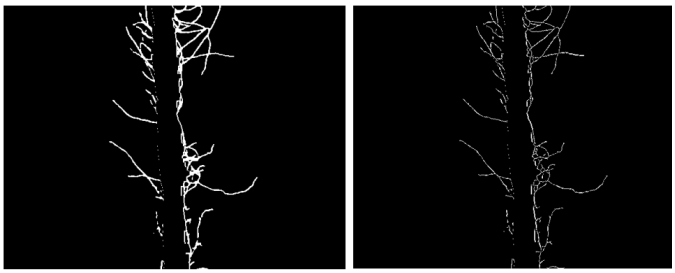

Figure 13. Initial image processing phase: (a) Result of subtracting the dilated image from the previously segmented image; (b) Result of applying the skeletonization operation to obtain the "skeleton" of the yarn.

Similar to the average diameter and defect detection methods, the pixel counting approach is used. The algorithm scans all pixels, storing the coordinates of white pixels (intensity 1) in a vector. After the scan, the stored pixel values are summed.
To calculate the hairiness coefficient, the total pixel area is determined by multiplying the number of white pixels by the real dimensions of the image. This area represents the loose fibers. The result is then divided by the represented yarn length to obtain hairiness per millimeter, which is later converted to meters [48-51].
Figure 14 presents the flowchart illustrating this methodology.

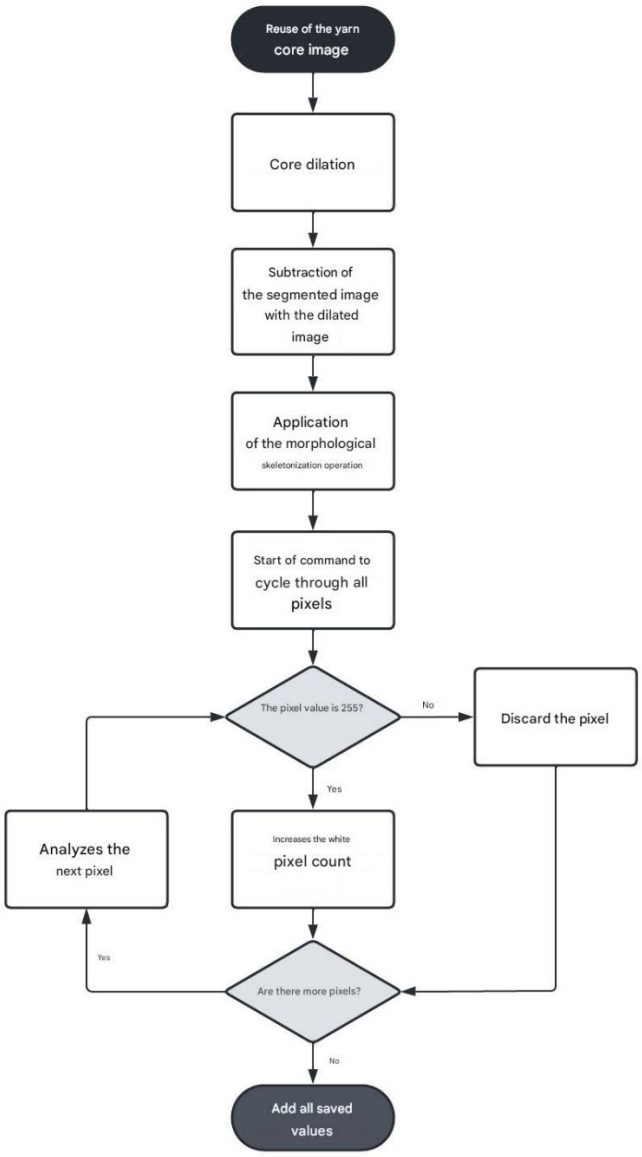

Figure 14. Flowchart of the methodology applied to obtain the hairiness coefficient.

In the current implementation, the hairiness coefficient is calculated by measuring the average radial distance of the fiber projections from the yarn core. Although this method captures the overall level of hairiness, it does not distinguish between straight, crossed, or curved fibers. As a result, some complex fiber geometries may be underrepresented. This is recognized as a limitation of the current system, and new techniques that can be used are described in Chapter 5 and future work using advanced segmentation techniques.

3.9. Twist Orientation and Twist Step

Twist is characterized by its direction (S or Z) and step. To extract these parameters, a new image is captured to better highlight the yarn's twist features, different from those analyzed previously.

The image undergoes initial processing steps:

(i) Grayscale conversion and Gaussian filtering to reduce color depth and primary noise.
(ii) Segmentation is applied using a higher manually adjusted threshold (value around 200) to isolate the twist patterns along the yarn core.
(iii) A morphological erosion operation is then used to remove residual noise and reduce the area of white pixels, improving object separation for analysis.

Figures 15a and 15b show the results after applying Otsu's algorithm [52-54] and morphological erosion.

Figure 15. Results obtained from the application of the algorithm: (a) Application of the Otsu algorithm for segmentation.; (b) Application of a morphological erosion operation.

Segmented objects are labeled to identify and count them. The twist direction is determined using PCA (Principal Component Analysis), which analyzes object orientation by identifying the dominant variation direction [55].

The logic applied is:

- Orientation < 90° → S-twist
- Orientation > 90° → Z-twist

Objects with insignificant areas are discarded, and the final twist direction is assigned based on the majority of detected orientations. Figure 16 illustrates the applied methodology.

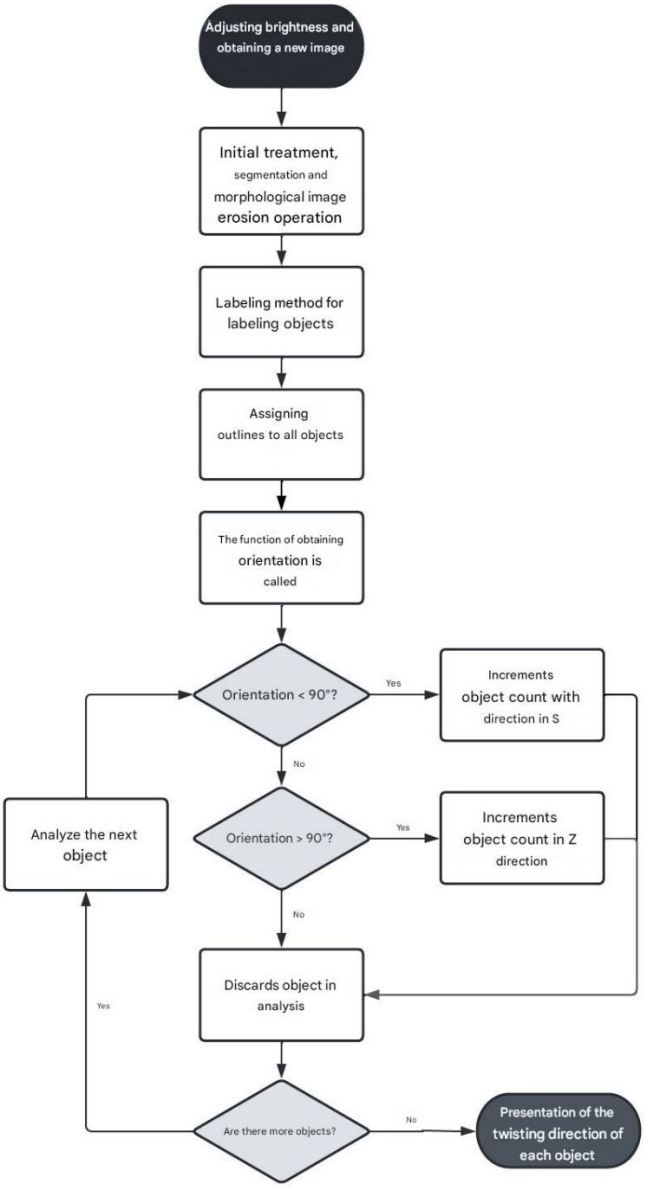

Figure 16. Flowchart for obtaining the twist direction.

The twist step is identified using the bounding box method, which assigns the smallest possible rectangle around each detected object [56]. This method calculates the rectangle based on the maximum and minimum pixel coordinates of each object, also determining the center, width, and height of each box—where the height corresponds to the twist pitch.

Two processing loops are used: one to assign bounding boxes to each object and another to draw them. The final average twist pitch is calculated from all measured objects. Figure 17 shows the conversion of detected twist sections into their corresponding bounding boxes.

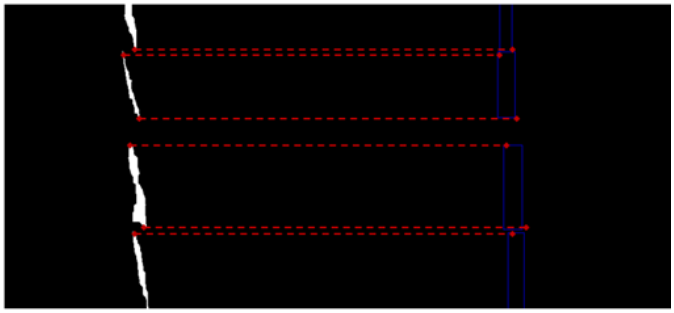

Figure 17. Assigning bounding boxes to different labeled objects.

The proposed hardware and software structure, combined with classical image processing techniques, allowed the collection of important parameters of the textile yarn. In the following chapter, the experimental results obtained through this system are presented and analyzed in detail, including a comparative evaluation with industrial reference systems.

4. Results and discussion

The aim of this chapter is to analyze the results obtained during the experimental tests. The yarn characteristics collected are compared with the results of the USTER Tester 3, except for the direction and twist pitch, whose objective was to evaluate the repeatability of the developed system. In general, brief conclusions are drawn based on the results obtained.

The strategy adopted to obtain the final results presented in this chapter was based on an incremental validation, initially using a set of 500 images for the main parameters and 50 for the analysis of the yarn twist. This approach, common in the initial phases of technological development, allowed demonstrating the technical feasibility of the system with errors of less than 7% in the parameters compared to the industrial equipment Uster Tester 3. Despite the reduced sample, the results confirm the quality of the adapted method. This methodology [57-60] recommends progressive validations in industrial contexts and with limited resources.

4.1. Extraction of linear mass, average diameter and specific volume

The extraction of the linear mass, mean diameter and specific volume parameters is based on the isolation of the yarn core after applying a morphological closing operation and a low-pass filter to remove loose fibers (hairiness). It is important to ensure that the morphological operation removes only the optimal amount of white pixels to avoid losing relevant information and preserve the yarn dimensions.

This condition was met for all three types of yarn analyzed, with a small residual noise in some cases, considered insignificant for the final results, as will be discussed later. Figures 18 to 20 illustrate samples A48 (purple cotton yarn), B226 (yellow cotton yarn) and C100 (white polyester yarn) before and after the application of the image processing techniques, showing the successful isolation of the yarn core.

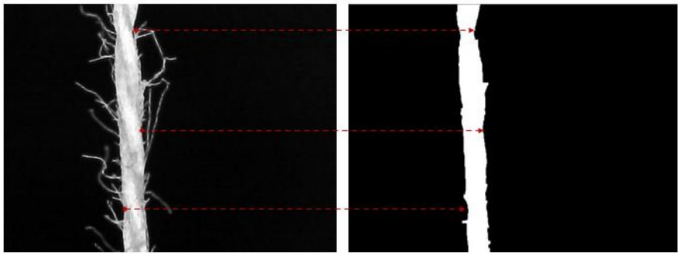

Figure 18. Result of the individualization of the core of sample A48.

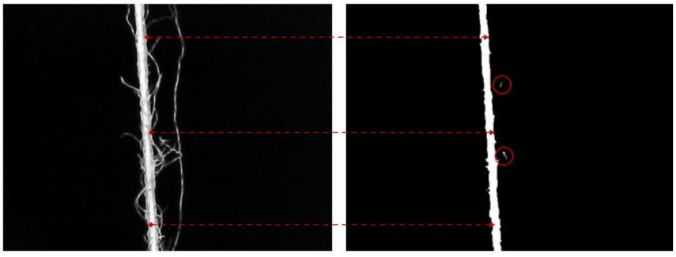

Figure 19. Result of the individualization of the core of sample B226.

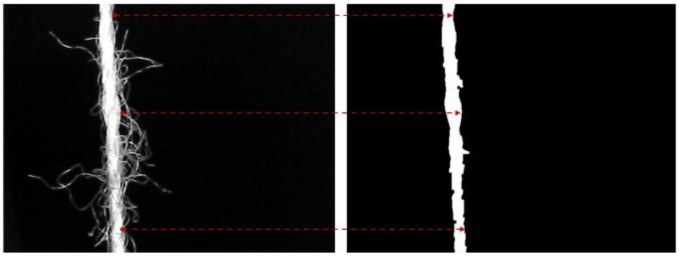

Figure 20. Result of the individualization of the core of sample C100.

In sample B226, a small residual noise remained after processing, as shown in Figure 19. Although this could be reduced by increasing the core size, this would question the dimensional accuracy of the wire and increase the computational cost. Therefore, the small noise level was considered acceptable, without affecting the final results.

Regarding the results obtained with the developed methodology, Table 4 presents the calculated values for the linear mass (g/km). For comparison purposes, the values measured by USTER Tester 3 and the corresponding percentage error are also provided.

Table 4. Results obtained for linear mass.

Linear Mass			
Yarn type	**System**	**Uster Tester System 3**	**Error Variation**
PURPLE COTTON	59,9 G/KM	56,4 G/KM	6,21%
YELLOW COTTON	25,4 G/KM	23,8 G/KM	6,66%
White Polyester	21,2 g/km	20,9 g/km	1,44%

The results in Table 4 show that the developed system achieved values for linear mass that are closely aligned with those obtained from the USTER Tester 3, with error variations remaining below 7% for all yarn types.

The highest deviation occurred with yellow cotton yarn (6.66%), likely due to its lower density and finer structure, which may introduce greater sensitivity to image processing imperfections. The purple cotton yarn presented a similar variation of 6.21%, remaining within an acceptable margin for industrial applications. The white polyester yarn showed the lowest error (1.44%), demonstrating high accuracy in linear mass estimation for synthetic materials, possibly due to their more uniform structure.

These results confirm the effectiveness of the proposed method in estimating linear mass with minimal deviation, validating its potential for low-cost, accurate quality control applications.

The average diameter and specific volume are mathematically related through the associated equations. Using the linear mass values from the USTER Tester 3, the results obtained with the developed system are generally satisfactory, as shown in Tables 5 and 6. The only exception is the specific volume for white polyester yarn, which shows a higher variation error. However, this is expected given the acceptable results already achieved for linear mass.

Table 5. Results obtained for the average diameter.

Average Diameter			
Yarn Type	**Developed System**	**USTER Tester 3**	**Error Variation**
COTTON PURPLE	0,290 MM	0,270 MM	7,40%
COTTON YELLOW	0,181 MM	0,177 MM	2,26%
POLYESTER WHITE	0,179 MM	0,177 MM	1,13%

Table 6. Results obtained for the specific volume.

Specific volume			
Yarn Type	**Developed System**	**USTER Tester 3**	**Error Variation**
COTTON PURPLE	1,06E-10 CM³/G	1,17E-10 CM³/G	9,40%
COTTON YELLOW	1,04E-10 CM³/G	1,08E-10 CM³/G	3,70%
POLYESTER WHITE	1,32E-10 CM³/G	1,21E-10 CM³/G	9,10%

The results presented in Tables 5 and 6 demonstrate that the developed system achieved a good level of accuracy for both the average diameter and specific volume across all yarn types.

For average diameter, the error variation remained low, especially for the polyester yarn (1.13%) and yellow cotton yarn (2.26%), indicating high measurement reliability. The slightly higher error for purple cotton yarn (7.40%) may be attributed to its larger diameter and structural variability, which introduces more complexity during image processing.

In the case of specific volume, the system achieved an error below 10% for all yarns, with the lowest error again observed for yellow cotton yarn (3.70%). Although the error for polyester yarn is slightly higher at 9.10%, it remains within acceptable limits for practical applications.

Overall, the results validate the effectiveness of the developed system, confirming its capability to estimate critical yarn parameters with minimal deviation from industrial benchmark equipment (USTER Tester 3).

4.2. Defect Extraction

Defect quantification uses the same image processing methods applied for calculating linear mass, average diameter, and specific volume. Defects are classified as:

- Thin places: mass variation below -50%.
- Thick places: mass variation above +50%.
- Neps: mass variation above +100%, adjusted to +200% to match the USTER Tester 3 standard.

This adjustment ensures better alignment with industrial measurements. The developed algorithm successfully identifies and visually classifies these defects, with results summarized in Table 7.

Table 7. Defects Identified by the Developed System and USTER Tester 3.

Yarn Type	Defects					
	Thin places		Tick places		Neps	
	System	USTER	System	USTER	System	USTER
COTTON PURPLE	0	0	15	0	1	0
COTTON YELLOW	14	67	31	10	17	25
POLYESTER WHITE	3	3	13	44	1	164

The results show that the developed system effectively detects defects, although some variations are observed when compared to the USTER Tester 3:

- For purple cotton yarn, the system identified only thick places (15 defects) and one nep, while the USTER detected none.
- In yellow cotton yarn, the system detected fewer thin places (14 vs 67) but more thick places (31 vs 10). Neps were also slightly undercounted (17 vs 25).
- For white polyester yarn, the system accurately matched the USTER in detecting thin places (3 defects) but significantly undercounted neps (1 vs 164), while detecting fewer thick places (13 vs 44).

Conclusion: The system reliably detects thin and thick places, but has limitations in identifying neps, particularly in synthetic yarns like polyester. This indicates that further refinement in image processing algorithms is needed to improve nep detection accuracy.
Next, Figure 21 illustrate examples of some of the defects identified.

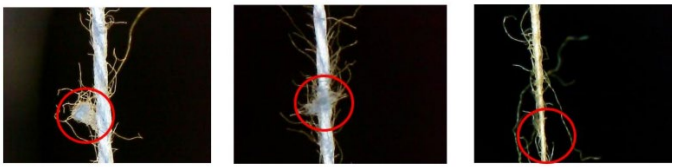

Figure 21. Some of the defects identified: (a) Nep identified in sample A91; (b) Thick place identified in sample A406; (b) Thin place identified in sample B301.

4.3. Hairiness Coefficient Extraction

Hairiness occurs when fibers protrude from the yarn core. In the developed algorithm, this parameter is analyzed through the hairiness coefficient, representing the amount of loose fibers per meter of yarn.
The method uses skeletonization to extract the yarn's structural outline, accurately identifying loose fibers, which are the focus of this analysis. Proper lighting is also highlighted as critical for accurate detection. Figure 22 show the results of applying this technique.

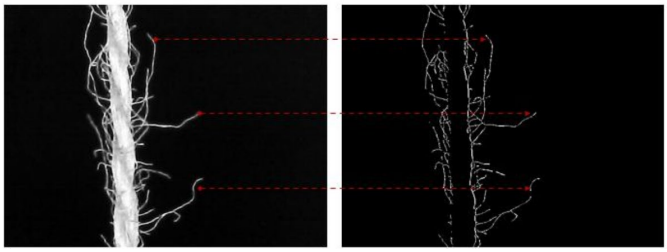

Figure 22. Result of the skeletonization of sample A25.

Table 8 allows you to compare the results obtained by the system created with the Uster Tester 3, which also show the respective variation error in relation to this.

Table 8. Results obtained for the hairiness coefficient.

Yarn Type	Hairiness coefficient		
	Developed System	USTER Tester 3	Error Variation
COTTON PURPLE	5,58	5,44	2,56%
COTTON YELLOW	5,21	4,77	9,22%
POLYESTER WHITE	3,61	3,31	8,31%

This difference is explained by the higher resolution and magnification capacity of the prototype's image analysis system compared to the USTER Tester 3. The developed system is capable of detecting even the finest protruding fibers, which may not be captured by the optical sensors used in the USTER Tester 3. As a result, the hairiness coefficient values obtained with the prototype tend to be slightly higher, especially for yarns with finer structures, such as yellow cotton and white polyester.
For the purple cotton yarn, the results show excellent agreement, with an error of only 2.56%, probably due to its larger diameter and dense fiber structure, which facilitates the detection of hairiness by both systems.
For yellow cotton and white polyester, the error variations are slightly higher (9.22% and 8.31%, respectively). This is due to the finer and more delicate structure of these yarns, where the prototype allows the detection of fine fibers that normally go unnoticed by the USTER Tester 3, due to the fact that it uses capacitive sensors.
Despite these differences, the system demonstrates good measurement capability and reliability, providing a more

detailed and comprehensive characterization of yarn hairiness. This makes it an interesting and cost-effective tool to help improve yarn and textile product quality control processes.

The yellow cotton yarn and the white polyester yarn present a combination of both types of hairiness, although loop fibers are the majority. Compared to the purple yarn, the loose fibers of these yarns are longer and are present in greater quantity along the length of the yarn. Figures 23 and 24 illustrate some examples of samples of these yarns with a higher hairiness density.

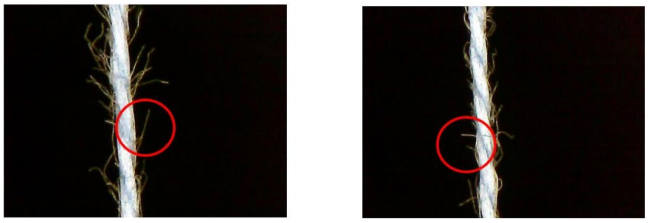

Figure 23. Protruding fibers in samples A103 and sample A376, respectively.

Figure 24. Loop fibers in samples B253 and C114, respectively.

4.4. Extraction of Twist Orientation and Twist step

The results for twist orientation or twist step are not compared with the USTER Tester 3, as this equipment does not provide these measurements. The validation of the developed algorithm for twist direction is performed through visual inspection of the captured samples. However, for twist pitch, visual validation is not possible; instead, the system's repeatability across multiple tests is analyzed.

Additionally, a new methodology was developed for extracting both parameters, requiring a different image acquisition process. This involves creating shadows along the yarn to highlight the twist patterns. Image processing then follows the previously established procedures.

Figures 25 illustrate the obtained results.

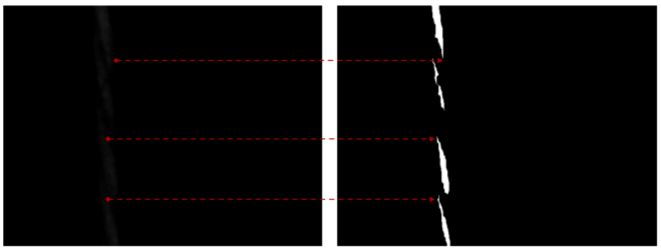

Figure 25. Result obtained from image processing for the twist study of sample 14 of the purple yarn.

The twist direction was determined using the Principal Components Analysis (PCA) statistical method, which identifies the most significant features of a dataset. In this case, PCA calculates the yarn's spatial orientation.

The twist direction is defined as follows:

- If the orientation is less than 90°, the twist is classified as S-twist.
- If the orientation is greater than 90°, the twist is classified as Z-twist.

Table 9 presents the results obtained for the twist orientation of each analyzed yarn type.

Table 9. Results obtained for the twist orientation.

Twist orientation		
Yarn type	**System**	**Representation**
PURPLE COTTON	S-TWIST	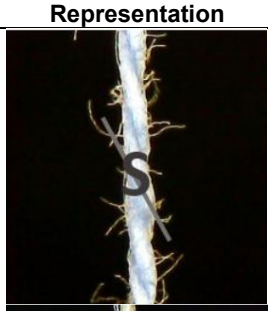
YELLOW COTTON	Z-TWIST	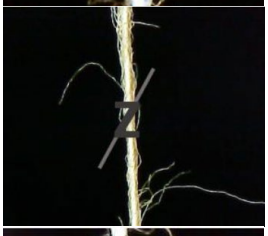
WHITE POLYESTER	Z-TWIST	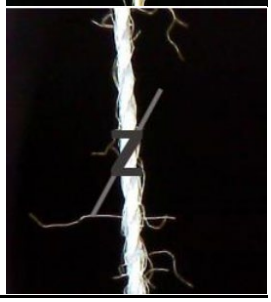

The twist direction assigned to each sample corresponds to the majority twist direction detected among the identified objects during image processing.
The algorithm correctly identified the twist direction for purple cotton yarn with a 100% accuracy rate and achieved an 82% accuracy rate for white polyester yarn, where 9 out of 50 samples were incorrectly classified.
Despite these occasional errors, the results are considered positive and confirm the system's effectiveness in determining twist direction.

This small difference is likely due to the following factors:

- **Material properties:** Polyester yarn tends to have a smoother, more reflective surface than cotton, making it difficult to enhance twist patterns during image acquisition. Shadows and contrasts essential for twist detection become less visible.
- **Illumination and shadow generation:** The methodology is based on the generation of shadows along the yarn to give relevance to twist patterns. This technique is most effective with rougher, more textured materials, such as cotton. In synthetic materials, light scattering reduces the sharpness of shadows, leading to incorrect detection of orientation.
- **High fiber uniformity:** Polyester yarns typically have a more uniform structure, which can make twist patterns less distinct in captured images, affecting the ability to correctly identify orientation.
- **Noise and influence of small objects:** In polyester samples, small artifacts or incomplete segmentation may have influenced the orientation calculations, leading to incorrect twist classification.

4.5 Economic Impact Assessment

One of the main advantages of the proposed system is its significant cost reduction compared to existing industrial solutions. The USTER Tester 3, an industry standard and widely used for yarn characterization, has an estimated acquisition cost of over €130,000.00, excluding maintenance and calibration expenses. On the other hand, the prototype developed in this work was assembled with a total hardware cost of less than €200, representing a cost reduction of over 99.85%. Despite the considerable cost difference, the proposed system demonstrated reliable performance, achieving error variations of less than 7% for linear mass and mean diameter, critical parameters for textile quality control. Furthermore, the system's high-resolution imaging and magnification capabilities allowed for a more detailed analysis of yarn hairiness, achieving better results depending on the detection capacity of the traditional optical and capacitive sensors of the USTER TESTER 3.
This economic advantage, combined with modularity and ease of implementation, makes the system interesting for small and medium-sized companies, research laboratories and educational environments. In addition, it allows for an affordable solution to improve quality control without the high investment typically required for this technology. The economic advantage of the developed system is clearly illustrated in Table 10, highlighting the substantial difference in acquisition costs between the two solutions.

Table 10. Cost Comparison Between Systems.

System	Acquisition Cost (€)	Maintenance Costs (€)	Measurement Capabilities
USTER TESTER 3	>100,000	HIGH	INDUSTRIAL STANDARD MEASUREMENTS
PROPOSED FRAMEWORK	<500	LOW (MINIMAL MAINTENANCE)	LINEAR MASS, DIAMETER, DEFECTS, HAIRINESS, TWIST

4.6. Discussion of Limitations

Although the proposed framework has demonstrated good performance in measuring the bulk parameters of textile yarns, some limitations have been identified:

- **Overestimation of hairiness detection:** Due to the high image resolution and high magnification, the system detects fine protruding fibers more effectively than the USTER Tester 3. This results in higher measured hairiness coefficients, especially for fine yarns such as yellow cotton and white polyester. Future work will address this issue by introducing machine learning models capable of distinguishing relevant protruding fibers from small surface irregularities.
- **Defect classification limitations:** The current system relies exclusively on classical image processing methods, which limits the accurate classification of complex defects such as neps. It is expected that incorporating AI-based defect classification can significantly improve this performance.
- **Environmental sensitivity:** Variations in lighting and external vibrations can affect the quality of image acquisition. Implementing adaptive lighting control and mechanical stabilization will help eliminate these issues.
- **Manual thresholding in some processes**: Certain processing steps, such as segmentation for twist analysis, still require manual threshold adjustments. Automation with AI-driven segmentation is an improvement that can be realized.

Despite these limitations, the system offers a cost-effective and reliable alternative for the inspection of industrial textile yarns, serving as a solid foundation for future technological improvements.

5. Conclusions and future work

This work presented a compact and low-cost system for analyzing yarn quality using classical image processing and accessible hardware. The system measures key parameters—linear mass, diameter, specific volume, hairiness coefficient, twist direction and pitch, and neps—using a single camera and open-source tools.

The method is based on a modular approach that allows simultaneous evaluation of multiple yarn properties in one setup. Validation against the Uster Tester 3 showed error rates below 7% for linear mass and diameter, confirming the method's reliability. Compared to commercial systems, this solution offers over 99% cost savings and is well suited for academic labs, small manufacturers, and teaching environments.

Some limitations remain, including the absence of coefficient of variation (CV) analysis for diameter and the detection of complex hairiness patterns. Future work will address these issues through:

- Integration of deep learning models for identifying and classifying defects (e.g., neps, hairiness);
- Manual control of parameters such as threshold values for twist analysis;
- Improved segmentation under varying lighting conditions using adaptive or AI-based techniques;
- Detection of crossed and curved hairiness with directional filters and neural networks;
- Estimation of diameter variation (CV) using machine learning or deep learning models.

Overall, this system offers a practical and extensible solution for yarn quality assessment, with clear potential for future improvement.

Acknowledgements.

The authors are grateful to engineer Joaquim Jorge, from the textile engineering department at the University of Minho, for all the support and availability given in this project.

References

[1] Yılmaz, K.; Aksu, İ.Ö.; Göçken, M.; Demirdelen, T. Sustainable Textile Manufacturing with Revolutionizing Textile Dyeing: Deep Learning-Based, for Energy Efficiency and Environmental-Impact Reduction, Pioneering Green Practices for a Sustainable Future. *Sustainability* **2024**, *16*, 8152. https://doi.org/10.3390/su16188152.

[2] Siliņa L, Dāboliņa I, Lapkovska E. Sustainable textile industry – wishful thinking or the new norm: A review. Journal of Engineered Fibers and Fabrics. 2024;19. doi: 10.1177/15589250231220359.

[3] Hamzi, A.; Habib, A.; Babaarslan, O.; Abushaega, M.M.; Masum, M.; al Mamun, M.A. Production of Sustainable Yarn Incorporating Process Waste to Promote Sustainability. *Processes* **2025**, *13*, 764. https://doi.org/10.3390/pr13030764.

[4] Filipe Pereira, Leandro Pinto, Filomena Soares, Rosa Vasconcelos, José Machado, Vítor Carvalho, Online yarn hairiness– Loop & protruding fibers dataset, Data in Brief, Volume 54, 2024, 110355, ISSN 2352-3409, https://doi.org/10.1016/j.dib.2024.110355.

[5] F. Pereira, V. Carvalho, F. Soares, R. Vasconcelos, J. Machado, 6 - Computer vision techniques for detecting yarn defects, Editor(s): W.K. Wong, In The Textile Institute Book Series, Applications of Computer Vision in Fashion and Textiles, Woodhead Publishing, 2018, Pages 123-145, ISBN 9780081012178, https://doi.org/10.1016/B978-0-08-101217-8.00006-3.

[6] Pereira, F., Carvalho, V., Vasconcelos, R., Soares, F. (2022). A Review in the Use of Artificial Intelligence in Textile Industry. In: Machado, J., Soares, F., Trojanowska, J., Yildirim, S. (eds) Innovations in Mechatronics Engineering. icieng 2021. Lecture Notes in Mechanical Engineering. Springer, Cham. https://doi.org/10.1007/978-3-030-79168-1_34.

[7] Wang L, Lu Y, Pan R, Gao W. Evaluation of yarn appearance on a blackboard based on image processing. *Textile Research Journal*. 2021;91(19-20):2263-2271. doi:10.1177/00405175211002863.

[8] Pereira, F., Oliveira, E.L., Ferreira, G.G., Sousa, F., Caldas, P. (2022). Textile Yarn Winding and Unwinding System. In: Machado, J., Soares, F., Trojanowska, J., Ottaviano, E. (eds) Innovations in Mechanical Engineering. icieng 2021. Lecture Notes in Mechanical Engineering. Springer, Cham. https://doi.org/10.1007/978-3-030-79165-0_33.

[9] Dai, N.; Jin, H.; Xu, K.; Hu, X.; Yuan, Y.; Shi, W. Prediction of Cotton Yarn Quality Based on Attention-GRU. *Appl. Sci.* **2023**, *13*, 10003. https://doi.org/10.3390/app131810003.

[10] Kopelmann, K.; Bruns, M.; Nocke, A.; Beitelschmidt, M.; Cherif, C. Characterization of the Viscoelastic Properties of Yarn Materials: Dynamic Mechanical Analysis in Longitudinal Direction. *Textiles* **2023**, *3*, 307-318. https://doi.org/10.3390/textiles3030021.

[11] Wang, H.; Han, Z.; Xiong, X.; Song, X.; Shen, C. Enhancing Yarn Quality Wavelength Spectrogram Analysis: A Semi-Supervised Anomaly Detection Approach with Convolutional Autoencoder. *Machines* **2024**, *12*, 309. https://doi.org/10.3390/machines12050309.

[12] Idzik, M.; Rybicki, T. Real-Time Prediction of the Yarn Break Position Using Vibration Measurement. *Sensors* **2025**, *25*, 299. https://doi.org/10.3390/s25020299.

[13] Rodrigues, M., Pereira, F., Machado, J. (2023). Analysis of Basic Characteristics of Textile Yarn Using Image Processing Techniques. In: Burduk, A., Batako, A., Machado, J., Wyczółkowski, R., Antosz, K., Gola, A. (eds) Advances in Production. ISPEM 2023. Lecture Notes in Networks and Systems, vol 790. Springer, Cham. https://doi.org/10.1007/978-3-031-45021-1_16.

[14] Caldas, P., Sousa, F., Pereira, F. *et al.* Automatic system for yarn quality analysis by image processing. *J Braz. Soc. Mech. Sci. Eng.* **44**, 565 (2022). https://doi.org/10.1007/s40430-022-03875-3.

[15] Deng, Z., Yu, L., Wang, L. *et al.* An algorithm for cross-fiber separation in yarn hairiness image processing. *Vis Comput* **40**, 3591–3599 (2024). https://doi.org/10.1007/s00371-023-03053-z.

[16] Gabriela, K., Jiří, M. Changes in hairiness of woven fabrics at the production and finishing stages. *Sci Rep* **15**, 2930 (2025). https://doi.org/10.1038/s41598-025-86610-x.

[17] Liu, Y.; Ge, C.; Su, Z.; Chen, Z.; Gao, C.; Gong, H.; Xu, W.; Xu, D.; Liu, K. Enhancing the Spun Yarn Properties by Controlling Fiber Stress Distribution in the Spinning Triangle with Rotary Heterogeneous Contact Surfaces. *Polymers* **2023**, *15*, 176. https://doi.org/10.3390/polym15010176.

[18] Hamzi, A.; Habib, A.; Babaarslan, O.; Abushaega, M.M.; Masum, M.; al Mamun, M.A. Production of Sustainable Yarn Incorporating Process Waste to Promote Sustainability. *Processes* **2025**, *13*, 764. https://doi.org/10.3390/pr13030764.

[19] Jedryka T. A Method for the Determination of Hairiness of Yarn. Textile Research Journal. 1963;33(8):663-665. doi:10.1177/004051756303300811.

[20] Krupincová, G., & Meloun, M. (2013). Yarn hairiness versus quality of yarn. *The Journal of The Textile Institute*, *104*(12), 1312–1319. https://doi.org/10.1080/00405000.2013.800377.

[21] A. Majumdar, 4 - Yarn hairiness and its reduction, Editor(s): R. Alagirusamy, A. Das, In Woodhead Publishing Series in Textiles, Technical Textile Yarns, Woodhead Publishing, 2010, Pages 112-139, ISBN 9781845695491, https://doi.org/10.1533/9781845699475.1.112.

[22] Z. Qiu, J. Wang and W. Gao, "A Computer-Vision-Based Nondestructive Hairiness Measurement System on Yarn Cone Transportation Line," in IEEE Transactions on Instrumentation and Measurement, vol. 73, pp. 1-13, 2024, Art no. 3512513, doi: 10.1109/TIM.2024.3372208.

[23] Guo, M., Gao, W. & Wang, J. Online Measurement of Sizing Yarn Hairiness Based on Computer Vision. *Fibers Polym* **24**, 1539–1552 (2023). https://doi.org/10.1007/s12221-023-00136-5.

[24] Pereira F, Lopes H, Pinto L, et al. Yarn quality analysis by using computer vision and deep learning techniques. *Textile Research Journal*. 2025;0(0). doi:10.1177/00405175251331205.

[25] Pereira, F.; Macedo, A.; Pinto, L.; Soares, F.; Vasconcelos, R.; Machado, J.; Carvalho, V. Intelligent Computer Vision System for Analysis and Characterization of Yarn Quality. *Electronics* **2023**, *12*, 236. https://doi.org/10.3390/electronics12010236.

[26] Zhang, H., Cheng, S., Zhao, Y., Jing, J., Su, Z., & Li, P. (2023). Measurement of yarn apparent evenness based on modified Canny edge detection. The Journal of The Textile Institute, 115(4), 600–606. https://doi.org/10.1080/00405000.2023.2201997.

[27] Zhang H, Zhu H, Yan K, Jing J, Su Z. Yarn apparent evenness detection based on L0 norm smoothing and the expectation maximization method. Textile Research Journal. 2022;93(1-2):422-433. doi:10.1177/00405175221119838.

[28] Z. Li et al., "3-D Measurement of Yarn Unevenness Based on A Low-Cost Multicamera Collaborative System and Signal Analysis," in IEEE Sensors Journal, vol. 24, no. 8, pp. 13343-13353, 15 April15, 2024, doi: 10.1109/JSEN.2024.3370629.

[29] Zhang, Huanhuan & Zhu, Houchun & Jing, Junfeng & Li, Pengfei & Pan, Quan. (2024). Curve-Like Structure Detection Using Multi-Sale and Boundary Assisted Segmentation Network. IEEE Transactions on Instrumentation and Measurement. PP. 1-1. 10.1109/TIM.2024.3350108.

[30] Li, Zhongjian & Pan, Ruru & Zhang, Jie & Li, Bianbian & Gao, Weidong & Bao, Wei. (2015). Measuring the unevenness of yarn apparent diameter from yarn sequence images. Measurement Science and Technology. 27. 015404. 10.1088/0957-0233/27/1/015404.

[31] Wang L, Xu B, Gao W. Multi-perspective measurement of yarn hairiness using mirrored images. Textile Research Journal. 2016;88(6):621-629. doi:10.1177/0040517516685281.

[32] Kulkarni, K.M., Sahu, A.R. (2022). Brief Overview on Study of Various Parameters Affecting the Productivity of Cotton Yarn. In: Kolhe, M.L., Jaju, S.B., Diagavane, P.M. (eds) Smart Technologies for Energy, Environment and Sustainable Development, Vol 1. Springer Proceedings in Energy. Springer, Singapore. https://doi.org/10.1007/978-981-16-6875-3_77.

[33] Patti, A.; Acierno, D. Materials, Weaving Parameters, and Tensile Responses of Woven Textiles. *Macromol* **2023**, *3*, 665-680. https://doi.org/10.3390/macromol3030037.

[34] Rotzler, S.; Malzahn, J.; Werft, L.; von Krshiwoblozki, M.; Eppinger, E. Influence of Knitting and Material Parameters on the Quality and Reliability of Knitted Conductor Tracks. *Textiles* **2022**, *2*, 524-545. https://doi.org/10.3390/textiles2040030.

[35] Kim, H.-A. Eco-Friendly Fibers Embedded Yarn Structure in High-Performance Fabrics to Improve Moisture Absorption and Drying Properties. *Polymers* **2023**, *15*, 581. https://doi.org/10.3390/polym15030581.

[36] Balakrishnan, N.K.; Siebert, S.; Richter, C.; Groten, R.; Seide, G. Effect of Colorants and Process Parameters on the Properties of Dope-Dyed Polylactic Acid Multifilament Yarns. *Polymers* **2022**, *14*, 5021. https://doi.org/10.3390/polym14225021.

[37] R. Pinto, F. Pereira, V. Carvalho, F. Soares and R. Vasconcelos, "Yarn linear mass determination using image processing: first insights," *IECON 2019 - 45th Annual Conference of the IEEE Industrial Electronics Society*, Lisbon, Portugal, 2019, pp. 198-203, doi: https://doi.org/10.1109/IECON.2019.8926650.

[38] Pereira, F.; Lopes, H.; Pinto, L.; Soares, F.; Vasconcelos, R.; Machado, J.; Carvalho, V. A Novel Deep Learning Approach for Yarn Hairiness Characterization Using an Improved YOLOv5 Algorithm. *Appl. Sci.* **2025**, *15*, 149. https://doi.org/10.3390/app15010149.

[39] Gorjanc, D.Š.; Sukič, N. Determination of Optimum Twist Equation for the Long Staple Combed Cotton Ring-Spun Yarn. *Fibers* **2020**, *8*, 59. https://doi.org/10.3390/fib8090059.

[40] Yu, C., Wu, W., Zheng, J. *et al.* A multi-stage adaptive otsu thresholding algorithm for pore segmentation in rock thin-section images. *Earth Sci Inform* **18**, 239 (2025). https://doi.org/10.1007/s12145-025-01716-0.

[41] Hirata, N.S.T.; Papakostas, G.A. On Machine-Learning Morphological Image Operators. *Mathematics* **2021**, *9*, 1854. https://doi.org/10.3390/math9161854.

[42] Wang, T.-K.; Yu, Y.-W.; Yang, T.-H.; Huang, P.-D.; Zhu, G.-Y.; Lau, C.-C.; Sun, C.-C. Depth Image Completion through Iterative Low-Pass Filtering. *Appl. Sci.* **2024**, *14*, 696. https://doi.org/10.3390/app14020696.

[43] BAŞER, GÜNGÖR. (2021). Determination of Yarn Diameter and Relevant Applications in Various Theoretical and Practical Problems. Tekstil ve Muhendis. 28. 134-148. 10.7216/1300759920212812207.

[44] Xu, Y., Hu, H., & Yuan, X. (2011). Geometrical analysis of co-woven knitted preform for composite reinforcement. *The Journal of The Textile Institute*, *102*(5), 405–418. https://doi.org/10.1080/00405000.2010.482346.

[45] Abdelkader, M. MATLAB Algorithms for Diameter Measurements of Textile Yarns and Fibers through Image

Processing Techniques. *Materials* **2022**, *15*, 1299. https://doi.org/10.3390/ma15041299.
[46] Haleem, N., Malik, Z.A., Malik, M.H. *et al.* Predicting the air permeability of polyester/cotton blended woven fabrics. *Fibers Polym* **14**, 1172–1178 (2013). https://doi.org/10.1007/s12221-013-1172-6.
[47] Valenzuela, W.; Saavedra, A.; Zarkesh-Ha, P.; Figueroa, M. Motion-Based Object Location on a Smart Image Sensor Using On-Pixel Memory. *Sensors* **2022**, *22*, 6538. https://doi.org/10.3390/s22176538.
[48] Fabijańska, A., Jackowska-Strumiłło, L. Image processing and analysis algorithms for yarn hairiness determination. *Machine Vision and Applications* **23**, 527–540 (2012). https://doi.org/10.1007/s00138-012-0411-y .
[49] Wang, T.; Yamakawa, Y. Edge-Supervised Linear Object Skeletonization for High-Speed Camera. *Sensors* **2023**, *23*, 5721. https://doi.org/10.3390/s23125721.
[50] Jaouadi, M., Msahli, S., & Sakli, F. (2009). Contribution to measurement of real yarn diameter. *The Journal of The Textile Institute*, *100*(2), 158–164. https://doi.org/10.1080/00405000701757487.
[51] Chandrasekaran, V., Senthilkumar, P. & Senthilkumar, M. Yarn Sample Preparation Techniques and Yarn Diameter Measurement for Analysing Cut-Cross Sectional View of Hollow Core Dref Spun Yarns. *J. Inst. Eng. India Ser. E* **95**, 89–95 (2014). https://doi.org/10.1007/s40034-014-0041-1.
[52] Liu, X.; Zhang, Z.; Hao, Y.; Zhao, H.; Yang, Y. Optimized OTSU Segmentation Algorithm-Based Temperature Feature Extraction Method for Infrared Images of Electrical Equipment. *Sensors* **2024**, *24*, 1126. https://doi.org/10.3390/s24041126.
[53] Zheng, J.; Gao, Y.; Zhang, H.; Lei, Y.; Zhang, J. OTSU Multi-Threshold Image Segmentation Based on Improved Particle Swarm Algorithm. *Appl. Sci.* **2022**, *12*, 11514. https://doi.org/10.3390/app122211514.
[54] Karakus, P. Detection of Water Surface Using Canny and Otsu Threshold Methods with Machine Learning Algorithms on Google Earth Engine: A Case Study of Lake Van. *Appl. Sci.* **2025**, *15*, 2903. https://doi.org/10.3390/app15062903.
[55] Gorjanc, D.Š.; Sukič, N. Determination of Optimum Twist Equation for the Long Staple Combed Cotton Ring-Spun Yarn. *Fibers* **2020**, *8*, 59. https://doi.org/10.3390/fib8090059.
[56] Ozkaya, Y. A., Acar, M., & Jackson, M. R. (2008). Yarn twist measurement using digital imaging. *The Journal of The Textile Institute*, *101*(2), 91–100. https://doi.org/10.1080/00405000802263476.
[57] Hevner A., et al. (2004) Design Science in Information Systems Research. MIS Quarterly, 28, 75-105. https://doi.org/10.2307/25148625.
[58] March, Salvatore. (1995). Design and Natural Sciences Research in Information Technology. Decision Support Systems. 15. 251-266. 10.1016/0167-9236(94)00041-2.
[59] Salvatore T. March, Gerald F. Smith, Design and natural science research in information technology, Decision Support Systems, Volume 15, Issue 4, 1995, Pages 251–266, ISSN 0167-9236, https://doi.org/10.1016/0167-9236(94)00041-2.
[60] Venable, J., Pries-Heje, J. & Baskerville, R. FEDS: a Framework for Evaluation in Design Science Research. Eur J Inf Syst 25, 77–89 (2016). https://doi.org/10.1057/ejis.2014.36.
[61] Bangare, Sunil & Dubal, Amruta Abasaheb & Bangare, Smit & Patil, Suhas. (2015). Reviewing Otsu's Method For Image Thresholding. International Journal of Applied Engineering Research. 10. 21777-21783. 10.37622/IJAER/10.9.2015.21777-21783.